Inorganic Chemistry

Article

pubs.acs.org/IC

Exploratory Investigation of New SHG Materials Based on Galloborates

Ting Hu,[†] Chun-Li Hu,[‡] Fang Kong,[‡] Jiang-Gao Mao,*[,‡] and Thomas C. W. Mak*[,†]

[†]Department of Chemistry and Center of Novel Functional Molecules, The Chinese University of Hong Kong, Shatin, New Territories, Hong Kong SAR, P. R. China

[‡]Fujian Institute of Research on the Structure of Matter, Chinese Academy of Sciences, Fuzhou, Fijian Province, P. R. China

Supporting Information

ABSTRACT: Three new galloborates, namely, $GaB_5O_8(OH)_2(en)_2{\cdot}H_2O$ (**1**), $LiGa(OH)(BO_3)(H_2O)$ (**2**), and $Rb_2Ga(B_5O_{10})(H_2O)_4$ (**3**), have been synthesized by hydrothermal reactions. Compound **1** is the first example of a galloborate that contains an organic component. It crystallizes in space group $P2_1/c$, and its crystal structure exhibits an infinite zigzag chain consisting of $[B_5O_8(OH)_2]^{3-}$ anions and GaO_2N_4 octahedra interconnected via corner sharing. Compound **2** crystallizes in space group $P31c$ with a layered structure composed of GaO_4, LiO_4, and BO_3 building units. Compound **3** belongs to chiral space group $C222_1$; the basic building blocks of the structure are the $[B_5O_{10}]^{5-}$ cluster anion and GaO_4 tetrahedron, which are interconnected to form a three-dimensional network with tunnels of Ga2B6 eight-membered rings (8-MRs) which are filled by Rb^+ cations and lattice water molecules. Interestingly, $Rb_2Ga(B_5O_{10})(H_2O)_4$ displays a moderate second-harmonic generation (SHG) response comparable to that of KH_2PO_4 (KDP), and it is phase matchable. Band structure and optical property calculations for $Rb_2Ga(B_5O_{10})(H_2O)_4$ based on DFT methods were also performed.

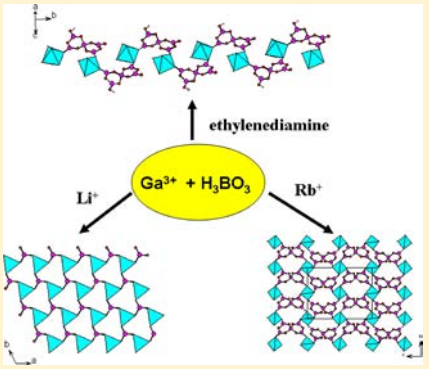

INTRODUCTION

Second-order nonlinear optical (NLO) materials have attracted much attention in recent years due to their wide applications in photonic technologies,[1] among which are inorganic crystals based on borates such as β-BaB_2O_4 and LiB_3O_5 and phosphates such as KH_2PO_4 (KDP) and $KTiOPO_4$ (KTP).[2]

The excellent nonlinear optical properties of borate crystals mainly originate from their anionic component, according to a theory proposed by Chen.[1b,3] Combination of a NLO-active anionic building unit with a π-conjugated system (such as BO_3^{3-}) and a polar group (such as an asymmetric metal−oxide polyhedron or a cationic coordination polyhedron possessing a lone pair) has been proved to be an effective route to synthesize new compounds with excellent second-harmonic generation (SHG) properties.[4] For example, introduction of the BeO_4 or BeO_3F tetrahedron into the borate system resulted in the discovery of several new deep-UV NLO crystals.[5]

The synergistic effect of lone pairs on Pb^{2+}, iodide, and the BO_3 and BO_4 groups produces a remarkably strong SHG response for $Pb_2B_5O_9I$ (SHG response ≈ 13.5 × KDP).[6] $Cd_4BiO(BO_3)_3$ with several types of asymmetric structural building units such as CdO_n, lone-pair active Bi^{3+}, and BO_3 groups also displayed a very large NLO coefficient (SHG response ≈ 6 × KDP).[7]

Introduction of the Ga^{3+} cation into the borate system is expected to afford many new types of compounds with various types of structures, since Ga^{3+} and B^{3+} ions have a similar outer electronic configuration, and both are able to adopt variable coordination geometries, such as trigonal planar BO_3 or tetrahedral BO_4 for B^{3+} and tetrahedral GaO_4 or octahedral GaO_6 for Ga^{3+}. These gallium borates may also display good SHG properties, for example, $Ba_4Ga_2B_8O_{18}Cl_2{\cdot}NaCl$, $BiAlGa_2(BO_3)_4$, and $Ba_2GaB_4O_9Cl$ display moderately strong SHG responses of about 1.0 ×, 4.0 ×, and 1.0 × KDP, respectively; furthermore, $BiAlGa_2(BO_3)_4$ is also found to be phase matchable.[8−10] Nevertheless, studies on compounds in this category are still rather limited.

Thus far most of the galloborates were synthesized by high-temperature solid-state reactions.[8−11] Some were prepared by the boric-acid flux method,[12] and $K_2[Ga(B_5O_{10})]{\cdot}4H_2O$ was prepared by a mild solvothermal method.[13] In order to better understand the structures and properties of the galloborates, we employed the hydrothermal method under mild conditions to obtain three new galloborates, namely, $GaB_5O_8(OH)_2(en)_2{\cdot}H_2O$ (**1**), $LiGa(OH)(BO_3)(H_2O)$ (**2**), and $Rb_2Ga(B_5O_{10})(H_2O)_4$ (**3**). Herein, we report their syntheses, crystal structures, and optical properties.

EXPERIMENTAL SECTION

Materials and Methods. All chemicals obtained from commercial sources were of analytically pure grade and used without further purification: H_3BO_3 (Beijing Chemical Works, 99.5%), Ga_2O_3 (Farco Chemical Supplies, 99.99%), Li_2CO_3 (International Laboratory,

Received: March 27, 2012
Published: July 31, 2012

   dx.doi.org/10.1021/ic3006376 | Inorg. Chem. 2012, 51, 8810−8817

99.5%), Rb_2CO_3 (Meryer, 99.9%), $Ga(NO_3)_3$ (Acros, 99.998%), diethylenetriamine (The British Drug Houses LTD, 0.95 g/mL), ethylenediamine (Riedel-de Haen AG, 98%). IR spectra were recorded on a Magna 750 FT-IR spectrometer as KBr pellets in the range of 4000−400 cm^{-1} with a resolution of 2 cm^{-1} at room temperature. X-ray powder diffraction (XRD) patterns were collected on a Rigaku MiniFlex II diffractometer using Cu Kα radiation in the angular range of 2θ = 5−65° with a step size of 0.02°. Optical diffuse reflectance and UV spectra were measured at room temperature with a Perkin-Elmer Lambda 900 UV−vis−NIR spectrophotometer using a $BaSO_4$ plate as a standard (100% reflectance). The absorption spectrum was calculated from reflectance spectra using the Kubelka−Munk function: $\alpha/S = (1 - R)^2/2R$, where α is the absorption coefficient, S is the scattering coefficient (which is practically wavelength independent when the particle size is larger than 5 μm), and R is the reflectance.[14] Thermogravimetric analyses (TGA) were carried out with a NETZCH STA449C unit at a heating rate of 15 °C min^{-1} under N_2 atmosphere, and differential scanning calorimetry (DSC) analyses were performed under N_2 on a NETZSCH DTA404PC unit at rate of 15 °C min^{-1} including the heating and cooling process. Measurements of the powder frequency-doubling effect were carried out on a sieved sample (70−100 mesh) by means of the modified method of Kurtz and Perry[15] using a fundament wavelength of 1064 nm generated by a Q-switched Nd:YAG laser. Sieved KDP (KH_2PO_4) sample in the same size range was used as a reference. Elemental analyses on C, H, and N elements for compound **1** were performed with a Vario MICRO CHNOS elemental analyzer. Elemental analyses for all three compounds were performed using an Ultima 2 inductively coupled plasma optical emission spectrometer (ICP-OES) with Sepex Certiprep standards.

Synthesis of $GaB_5O_8(OH)_2(en)_2{\cdot}H_2O$ (1). A mixture of H_3BO_3 (0.618 g, 10 mmol), Ga_2O_3 (0.060 g, 0.32 mmol), and ethylenediamine (1 mL) was stirred continuously for 2 h at room temperature. The final mixture was sealed in an autoclave equipped with a Teflon liner (23 mL) and heated at 160 °C for 50 h followed by slow cooling to room temperature at a rate of 2 °C/h. The initial and final pH values of the solution were about 9 and 8, respectively. The product was washed with hot water and ethanol and then dried in air. Colorless brick-shaped crystals of **1** were isolated in ∼79.3% yield. Its purity was confirmed by XRD powder diffraction study (see Figure S1a in the Supporting Information). Anal. Calcd for $C_4H_{20}B_5GaN_4O_{11}$: C, 11.33; H, 4.75; N, 13.21; Ga, 16.44; B, 12.75. Found: C, 10.20; H, 4.45; N, 12.79; Ga, 16.76; B, 12.14. IR data (KBr cm^{-1}): 3240(s), 2965(m), 2360(w), 1602(m), 1360(s), 1240(s), 1040(s), 931(m), 799(w), 711(w), 612(w), 535(w).

Synthesis of $LiGa(OH)(BO_3)(H_2O)$ (2). A mixture of H_3BO_3 (0.2 g, 3.2 mmol), Ga_2O_3 (0.060 g, 0.32 mmol), Li_2CO_3 (0.070 g, 1 mmol), diethylenetriamine (0.5 mL), and H_2O (0.5 mL) was stirred continuously for 2 h at room temperature. Diethylenetriamine here served to raise the pH, as Ga_2O_3 is more soluble in an alkaline environment. The final mixture with a pH value of 8−9 was sealed in an autoclave equipped with a Teflon liner (23 mL), heated at 160 °C for 50 h, and then slowly cooled to room temperature at a rate of 4 °C/h. The final pH value of the reaction media was about 8. The product was washed with hot water and ethanol and then dried in air. Colorless hexagonal tile-shaped crystals of **2** were obtained. Many attempts were tried to prepare a pure product by changing reaction times and temperatures as well as the ratios of reactant reagents; however, some unidentified impurity always appeared. A sample composed of manually selected single crystals was used for ICP-EA analysis. Anal. Calcd for H_3BO_5GaLi: Li, 4.07; Ga, 40.89; B, 6.34. Found: Li, 4.59; Ga, 39.51; B, 6.01. Other characterization procedures such as SHG property, TGA, and IR measurements were not performed due to the lack of enough samples available.

Synthesis of $Rb_2Ga(B_5O_{10})(H_2O)_4$ (3). A mixture of H_3BO_3 (0.2 g, 3.2 mmol), Rb_2CO_3 (0.074 g, 0.32 mmol), $Ga(NO_3)_3$ (0.080 g, 0.32 mmol), diethylenetriamine (0.5 mL), and H_2O (0.5 mL) was stirred continuously for 2 h at room temperature. Diethylenetriamine was also added as an alkalizing agent. The mixture with a pH value of 8−9 was sealed in an autoclave equipped with a Teflon liner (23 mL), heated at 160 °C for 50 h, and finally slow cooled to room temperature at a rate of 4 °C/h. The final pH value of the reaction media was about 8. The product was washed with hot water and ethanol and then dried in air. Colorless rhombohedral crystals of **3** were collected in ∼41% yield. Its purity was confirmed by XRD powder diffraction study (Figure S1b in the Supporting Information). Energy-dispersive spectrometry (EDS) elemental analyses on several single crystals of **3** gave an average molar ratio of Rb:Ga of 5.3:2.6, which is in good agreement with that determined from single-crystal X-ray structural studies. ICP analyses calcd for $H_8B_5GaO_{14}Rb_2$: Rb, 32.45; Ga, 13.24; B, 10.26. Found: Rb, 31.88; Ga, 12.48; B, 9.51. IR data (KBr cm^{-1}): 3524(s), 2919(w), 2348(w), 1666(w), 1358(s), 1237(s), 1050(w), 940(m), 808(w), 726(w), 635(w), 542(w).

Single-Crystal Structure Determination. Crystal data were collected on a Bruker Smart Apex II CCD diffractometer with Mo Kα radiation (λ = 0.71073 Å) at 293(2) K. All three data sets were corrected for Lorentz and polarization factors, as well as for absorption by the multiscan method.[16] All three structures were solved by direct methods and refined by full-matrix least-squares fitting on F^2 by SHELX-97.[17] All non-hydrogen atoms were refined with anisotropic thermal parameters. In **1**, atoms O(1) and O(7) are assigned to hydroxyl groups based on the requirement of charge balance and bond valence calculations; their calculated bond valences are −1.04 and −1.03, respectively.[18] In **2**, atoms O(1) and O(2) are assigned to a hydroxide anion and an aqua ligand, respectively, based on the requirement of charge balance and bond valence calculations; their calculated bond valences are −0.776 and −0.289, respectively.[18] All hydrogen atoms except those associated with water molecules in compound **3** are introduced at geometrically calculated positions and refined with isotropic thermal parameters. H(1wa), H(2wa), H(3wa), and H(3wb) in compound **3** were located from difference Fourier maps and refined with isotropic thermal parameters. For non-centrosymmetric **2** (space group $P31c$) and **3** ($C222_1$), their Flack parameters were refined to 0.11(4) and 0.12(1), respectively, indicating the existence of a small degree of racemic twinning. Structures were also checked for possible missing symmetry with PLATON.[19] Crystallographic data and structural refinements for the two compounds are summarized in Table 1. Important bond distances are listed in Table 2. More details on the crystallographic studies as well as atomic displacement parameters are given as Supporting Information.

Computational Study. Single-crystal structural data of **3** was used for the theoretical calculations. The band structure, density of states (DOS), and optical properties were performed with the total-energy code CASTEP.[20] The total energy was calculated with density functional theory (DFT) using the Perdew−Burke−Ernzerhof (PBE) generalized gradient approximation.[21] The interactions between the ionic cores and the electrons were described by the norm-conserving pseudopotential.[22] The following valence-electron configurations were considered in the computation: Rb-$4s^24p^65s^1$, Ga-$3d^{10}4s^24p^1$, B-$2s^22p^1$, O-$2s^22p^4$, and H-$1s^1$. The number of plane waves included in the basis sets was determined by a cutoff energy of 800 eV, and numerical integration of the Brillouin zone was performed using a Monkhorst−Pack k-point sampling of 3 × 3 × 2 for the compound. The other parameters and convergence criteria were the default values of the CASTEP code.

Calculations of linear optical properties in terms of the complex dielectric function $\varepsilon(\omega) = \varepsilon_1(\omega) + i\varepsilon_2(\omega)$ were made. The imaginary part of the dielectric function ε_2 was given in the following equation[23]

$$\varepsilon_2^{ij}(\omega) = \frac{8\pi^2\hbar^2e^2}{m^2V}\sum_k\sum_{cv}(f_c - f_v)\frac{p_{cv}^i(k)p_{vc}^j(k)}{E_{vc}^2}$$
$$\delta[E_c(k) - E_v(k) - \hbar\omega] \quad (1)$$

where f_c and f_v represent the Fermi distribution functions of the conduction and valence bands, respectively. The term $p_{cv}^i(k)$ denotes the momentum matrix element transition from the energy level c of the conduction band to the level v of the valence band at a certain k point in the Brillouin zones, and V is the volume of the unit cell. The

dx.doi.org/10.1021/ic3006376 | Inorg. Chem. 2012, 51, 8810−8817

Table 1. Crystal Data and Structure Refinements for $GaB_5O_8(OH)_2(en)_2{\cdot}H_2O$, $LiGa(OH)(BO_3)(H_2O)$, and $Rb_2Ga(B_5O_{10})(H_2O)_4$

	$GaB_5O_8(OH)_2(en)_2{\cdot}H_2O$	$LiGa(OH)(BO_3)(H_2O)$	$Rb_2Ga(B_5O_{10})(H_2O)_4$
formula	$C_4H_{20}B_5N_4O_{11}Ga$	H_3BO_5GaLi	$H_8B_5GaO_{14}Rb_2$
fw	424.01	170.50	526.77
space group	$P2_1/c$ (No.14)	$P31c$ (No. 159)	$C222_1$ (No. 20)
a (Å)	9.302(4)	4.83(2)	9.54(6)
b (Å)	12.332(6)	4.83(2)	10.38(5)
c (Å)	14.315(7)	12.03(1)	14.03(9)
α (deg)	90	90	90
β (deg)	96.11(1)	90	90
γ (deg)	90	120	90
V (Å^3)	1632.90(1)	243.30	1389.58(1)
Z	4	2	4
D_c (g·cm^{-3})	1.725	2.327	2.518
μ(Mo Kα) (mm^{-1})	1.746	5.568	9.008
GOF on F^2	1.035	1.097	1.068
Flack factor	none	0.11(4)	0.12(1)
R1, wR2 [$I > 2\sigma(I)$][a]	0.0248, 0.0640	0.0298, 0.0671	0.0266, 0.0684
R1, wR2 (all data)[a]	0.0292, 0.0672	0.0316, 0.0686	0.0267, 0.0685

[a] $R1 = \sum||F_o| - |F_c||/\sum|F_o|$, $wR2 = \{\sum w[(F_o)^2 - (F_c)^2]^2/\sum w[(F_o)^2]^2\}^{1/2}$.

symbols m, e, and $\hbar$ represent the electron mass, charge, and Plank's constant, respectively.

The second-order optical properties were calculated based on the momentum-gauge formalism with the minimal-coupling interaction Hamiltonian and within the independent-particle approximation.[24] The imaginary part of the frequency-dependent second-order susceptibility $\chi^{(2)}(2\omega, \omega, \omega)$ was obtained using the expressions given elsewhere.[25] The Kramers–Kronig relations, as required by causality, were used to obtain the real part

$$\chi'^{(2)}(-2\omega, \omega, \omega) = \frac{2}{\pi} P \int_0^\infty d\omega' \frac{\omega' \chi''^{(2)}(2\omega', \omega', \omega')}{\omega'^2 - \omega^2} \quad (2)$$

In the present study, the δ function in the expressions for $\chi^{(2)}(2\omega, \omega, \omega)$ was approximated by a Gaussian function with $\Gamma = 0.2$ eV. Furthermore, to ensure reliability of the real part calculated via the Kramer–Kronig transformation (eq 2) at least 500 empty bands were used in SHG calculation.

RESULTS AND DISCUSSION

Three new gallium borates, $GaB_5O_8(OH)_2(en)_2{\cdot}H_2O$ (**1**), $LiGa(OH)(BO_3)(H_2O)$ (**2**), and $Rb_2Ga(B_5O_{10})(H_2O)_4$ (**3**), have been successfully synthesized by the hydrothermal method. They exhibit three types of novel galloborate anionic architectures. Compound **1** is the first gallium borate bearing an organic component. Compound **3** displays moderate second-harmonic generation efficiencies that are comparable to KH_2PO_4(KDP). It should be stressed that **2** and **3** could not be synthesized in the absence of triethylenediamine, which presumably functions as a mediator of the pH value. The presence of base is necessary to avoid protonation of the borate group, which usually occurs in an acidic medium. Ga_2O_3 is insoluble in water at room temperature, but it can be dissolved in a basic solution under hydrothermal condition. During preparation of compounds **2** and **3**, other nitrogen bases such as pyridine and ethylenediamine were tried instead of triethylenediamine but success remained elusive. The reason why triethylenediamine plays a unique role in generating compounds **2** and **3** is still unknown.

Table 2. Important Bond Lengths (Angstroms) for $GaB_5O_8(OH)_2(en)_2{\cdot}H_2O$ (1), $LiGa(OH)(BO_3)(H_2O)$ (2), and $Rb_2Ga(B_5O_{10})(H_2O)_4$ (3)[a]

bond	length	bond	length
compound **1**			
Ga(1)–O(4)#1	1.924 (1)	B(3)–O(9)	1.464(2)
Ga(1)–O(10)	1.942(1)	B(3)–O(5)	1.466(2)
Ga(1)–N(2)	2.075(1)	B(3)–O(2)	1.473(2)
Ga(1)–N(3)	2.092(2)	B(3)–O(6)	1.478(2)
Ga(1)–N(4)	2.119(1)	B(4)–O(6)	1.355(2)
Ga(1)–N(1)	2.164(1)	B(4)–O(7)	1.360(2)
B(1)–O(4)	1.337(2)	B(4)–O(8)	1.388(2)
B(1)–O(5)	1.360(2)	B(5)–O(10)	1.341(2)
B(1)–O(3)	1.413(2)	B(5)–O(9)	1.365(2)
B(2)–O(2)	1.357(2)	B(5)–O(8)	1.414(2)
B(2)–O(1)	1.357(2)	B(2)–O(3)	1.379(2)
compound **2**			
Li(1)–O(2)	1.933(1)	Ga(1)–O(3)	1.832(3)
Li(1)–O(3)	1.931(6)	Ga(1)–O(1)	1.826(5)
B(1)–O(3)	1.363(3)		
compound **3**			
Rb(1)–O(1W)	2.916(4)	Rb(1)–O(5)#1	2.952(3)
Rb(1)–O(2)#2	2.972(3)	Rb(1)–O(3)#1	2.971(3)
Rb(1)–O(3W)#3	2.985(5)	Rb(1)–O(4)#4	3.035(3)
Rb(1)–O(3W)	3.163(9)	Rb(1)–O(1)	3.189(3)
Rb(1)–O(2W)#5	3.446(3)	Ga(1)–O(5)#6	1.820(3)
Ga(1)–O(5)#7	1.820(3)	Ga(1)–O(4)	1.821(2)
Ga(1)–O(4)#8	1.821(2)	B(1)–O(2)	1.4561(5)
B(1)–O(2)#2	1.461(5)	B(1)–O(1)#2	1.476(5)
B(1)–O(1)	1.476(5)	B(2)–O(5)	1.346(6)
B(2)–O(2)	1.356(5)	B(2)–O(3)	1.393(5)
B(3)–O(4)	1.347(5)	B(3)–O(1)	1.372(5)
B(3)–O(3)	1.376(5)		

[a] Symmetry transformations used to generate equivalent atoms: For **1**: #1, $-x+2, y-1/2, -z+1/2$. For **3**: #1 $-x+3/2, -y+3/2, z+1/2$; #2 $-x+2, y, -z+3/2$; #3 $-x+1, y, -z+3/2$; #4 $-x+3/2, y-1/2, -z+3/2$; #5 $x+1/2, y+1/2, z$; #6 $x-1/2, -y+3/2, -z+1$; #7 $x-1/2, y+1/2, z$; #8 $x, -y+2, -z+1$.

Description of the Crystal Structure. $GaB_5O_8(OH)_2(en)_2{\cdot}H_2O$ (**1**) crystallizes in centrosymmetric monoclinic space group $P2_1/c$ (No. 14) with $Z = 4$. The Ga^{3+} ion is octahedral coordinated by two chelating bidentate ethylenediamine ligands and two oxygen atoms from two $[B_5O_8(OH)_2]^{3-}$ anions (Figure 1a). The Ga–O distance are in the range of 1.9241(1)–1.941(1) Å, and the Ga–N distances are in the range of 2.075(1)–2.164(1) Å. The O–Ga–O bond angle is 89.84(5)°. Within the $[B_5O_8(OH)_2]^{3-}$ anion, atoms B1, B2, B4, and B5 exhibit typical trigonal-planar coordination with B–O distances in the range of 1.337(2)–1.414(2) Å and O–B–O bond angles in the range of 115.7(1)–123.8(1)°. The central atom B(3) is tetrahedrally coordinated with B–O distances in the range of 1.464(2)–1.478(2) Å and O–B–O bond angles in the range of 108.4(1)–110.8(1)°. These bond length and angles are comparable to those previously reported in related gallium borates.[8−13] Neighboring gallium(III) ions are bridged by $[B_5O_8(OH)_2]^{3-}$ clusters into an infinite zigzag chain along the b axis (Figure 1b). The lattice water molecule O1W is located in the interchain region and form donor hydrogen bonds with hydroxyl group O7 and bridging oxygen

dx.doi.org/10.1021/ic3006376 | Inorg. Chem. 2012, 51, 8810–8817

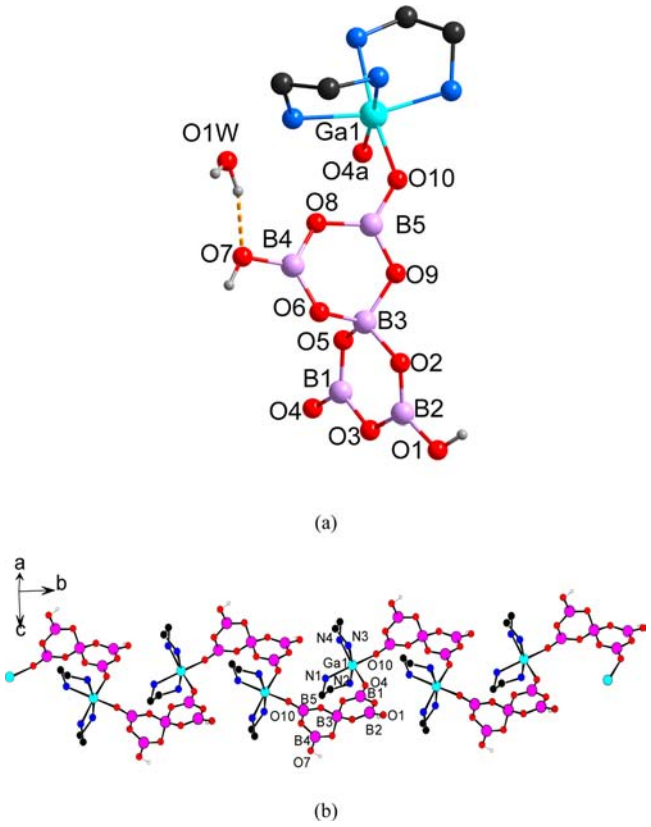

Figure 1. (a) Asymmetric unit of $GaB_5O_8(OH)_2(en)_2{\cdot}H_2O$ (**1**). Hydrogen bond between the lattice water molecule O1W and O7 is presented by a broken yellow line. (b) Infinite zigzag coordination chain along the *b* axis. Hydrogen atoms of the ethylenediamine ligands are omitted for clarity. Ga, N, B, O, C, and H atoms are drawn as light blue, dark blue, purple, red, black, and gray circles, respectively. Symmetry codes: a $2 - x, -0.5 + y, 0.5 - z$.

atom O9 of the $[B_5O_8(OH)_2]^{3-}$ cluster (O1W···O7, 2.78; O1W···O9a, 3.00; a $x, 1.5 - y, 0.5 + z$).

$LiGa(OH)(BO_3)(H_2O)$ (**2**) crystallizes in noncentric trigonal space group *P*31*c* (No. 159) with $Z = 3$. The BO_3 and OH groups, Li^+ and Ga^{3+} ions, and the H_2O molecule all occupy special positions of site symmetry 3, so that the H atoms necessarily exhibit orientational disorder. The Ga^{3+} ion is tetrahedrally coordinated by three oxygen atoms from three BO_3 group and a hydroxide anion (Figure 2a). Ga–O distances are 1.824(6) (Ga1–O1) and 1.831(4) Å (Ga1–O3). O–Ga–O bond angles are 110.0(1)° (O1–Ga1–O3) and 108.9(1)° (O3–Ga1–O3). These bond lengths and angles are comparable to those previously reported in related gallium borates.[8−13] Within the trigonal-planar BO_3 group the B–O bond length and O–B–O bond angle are 1.364(4) Å and 119.96(4)°, respectively. The GaO_4 and BO_3 groups are alternatively interconnected via corner sharing into a layer with B_3Ga_3 6-MRs (Figure 2b). The Li^+ ions are located at the centers of the B_3Ga_3 rings to form a honeycomb-like lithium galloborate layer paralleled to the *ab* plane (Figure 2c). The Li^+ ion is tetrahedrally coordinated by three oxygen atoms from three BO_3 groups and an aqua ligand. Li–O bond lengths are 1.93(1) (Li1–O2) and 1.93(6) Å (Li1–O3), and O–Li–O bond angles are 113.4(4)° (O2–Li1–O3) and 105.3(4)° (O3–Li1–O3). The honeycomb-like layers are held together via weak hydrogen bonds among hydroxide anions and aqua

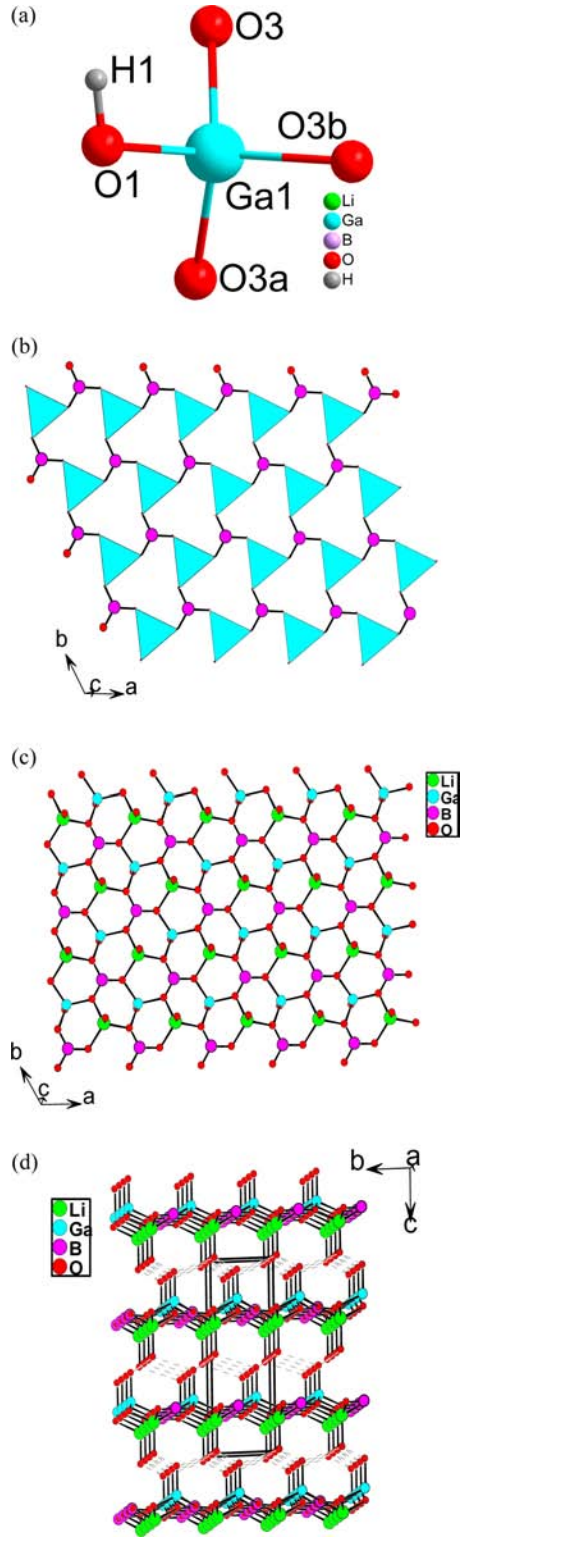

Figure 2. (a) Coordination environment of the Ga atom in $LiGa(OH)(BO_3)(H_2O)$ (**2**). (b) Galloborate layer composed of linked GaO_4 tetrahedra and trigonal-planar BO_3 groups parallel to the *ab* plane. (c) Lithium galloborate layer composed of LiO_4, GaO_4 tetrahedra, and BO_3 groups parallel to the *ab* plane. Note that the two kinds of tetrahedra point in opposite directions along the *c* axis. (d) Crystal structure of **2** viewed along the *a* axis. Hydrogen bonds are drawn as dashed lines. Li, Ga, B, O, and H atoms are drawn as green, light blue, purple, red, and gray circles, respectively. GaO_4 polyhedra are shaded in light blue. Symmetry codes: a $1 - x + y, -x, z$; b $-y, -1 + x - y, z$; c $-1 + x, y, 0.5 + z$.

dx.doi.org/10.1021/ic3006376 | *Inorg. Chem.* 2012, 51, 8810–8817

ligands (O1···O2 2.923 Å) into a three-dimensional network (Figure 2d).

$Rb_2Ga(B_5O_{10})(H_2O)_4$ (**3**) crystallizes in chiral space group $C222_1$ (No. 20) with $Z = 4$. In the unit cell, the Ga^{3+} ion, $[B_5O_{10}]^{5-}$ cluster, and two water molecules each lie on a crystallographic 2-fold axis whereas the Rb^+ ion and one water molecule occupy general positions. The crystal structure features a novel 3D anionic network composed of Ga^{3+} ions and $[B_5O_{10}]^{5-}$ clusters with voids filled by Rb^+ ions and water molecules (Figure 3a). The Ga^{3+} ion is tetrahedrally coordinated by four oxygen atoms from four different B_5O_{10} groups. Ga−O distances are 1.819(3) (Ga1−O5) and 1.821(3) Å (Ga1−O4). O−Ga−O bond angles fall in the range from 105.2(3)° to 116.5(2)°. The $[B_5O_{10}]^{5-}$ anion has the same structure as those reported previously,[13,26] being composed of three BO_3 triangles and one BO_4 tetrahedron. The B−O bond lengths of BO_3 groups are in the range from 1.354(6) to 1.394(6) Å, and the O−B−O angles are in the range from 116.3(4)° to 124.0(4)°. B−O bond lengths of BO_4 groups are in the range from 1.463(5) to 1.471(5) Å, and O−B−O angles are in the range from 108.2(5)° to 110.9(2)°. The GaO_4 tetrahedra and $[B_5O_{10}]^{5-}$ anions are interconnected to form a three-dimensional framework (Figure 3a). Viewed along the *a* axis, there are two types of open tunnels based on Ga_2B_4 6-MRs and Ga_2B_6 8-MRs, respectively. The rubidium cations and solvated water molecules are located in the 8-MR channels (Figure 3a). The Rb^+ ion is 9-coordinated by five oxygen atoms from three $[B_5O_{10}]^{5-}$ anions and four aqua ligands. The Rb−O distances fall in the range from 2.918(4) to 3.446(3) Å. The lattice water molecules are linked to the crystal skeleton through hydrogen bonding (of type O1W···O4, 3.025; O2W···O5, 3.13; O3W···O2W, 2.81).

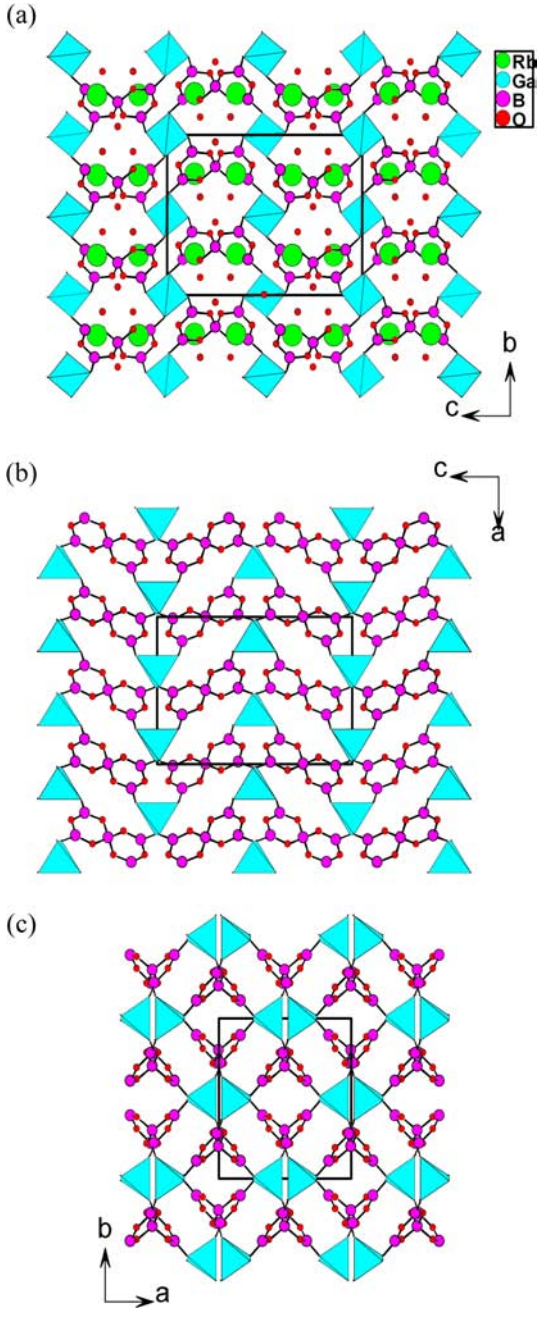

Figure 3. (a) View of the crystal structure of $Rb_2Ga(B_5O_{10})(H_2O)_4$ (**3**) along the *a* axis. (b) Anionic network viewed along the *b* axis. (c) Anionic network viewed along the *c* axis. Rb, Ga, B, and O atoms are drawn as green, light blue, purple, and red circles, respectively. GaO_4 polyhedra are shaded in light blue.

It is interesting to note that when viewed along the *b* and *c* axes, the 3D anionic network of $Rb_2Ga(B_5O_{10})(H_2O)_4$ also displays two types of 1D tunnels based on Ga_2B_6 8-MRs and Ga_2B_4 6-MRs, respectively (Figure 3b and 3c). Though the ring systems are similar, the shapes of the tunnels are different depending on the viewing axial directions.

TGA Studies. TGA studies indicate that there is a relatively slow weight loss for $GaB_5O_8(OH)_2(en)_2{\cdot}H_2O$ in the range of 70−200 °C, which corresponds to release of 1 mol of lattice H_2O molecules per formula unit. The observed weight loss of 4.73% well matches with the calculated one (4.25%) (Figure S2a in the Supporting Information). In the temperature range of 300−1200 °C, $GaB_5O_8(OH)_2(en)_2{\cdot}H_2O$ loses weight continually due to release of the organic amine and water. If the final residue is assumed to be GaB_5O_9, the observed total weight loss of 34.0% is significantly smaller than the calculated value (36.85%); hence, decomposition of $GaB_5O_8(OH)_2(en)_2{\cdot}H_2O$ is not complete even at 1200 °C. $Rb_2Ga(B_5O_{10})(H_2O)_4$ exhibits one step of weight loss in the range of 40−200 °C, which corresponds to release of 4 mol of H_2O molecules per formula unit (Figure S2b in the Supporting Information). The observed weight loss of 13.0% well matches with the calculated one (13.7%). After dehydration, the compound becomes amorphous and lost weight slowly in the range of 200−800 °C. The final residuals were not characterized since the residuals melted and were stuck to the TGA bucket, which is made of Al_2O_3 for use at such high temperatures.

Optical Properties and Vibrational Spectra. Optical diffuse reflectance spectra revealed that both $GaB_5O_8(OH)_2(en)_2{\cdot}H_2O$ (**1**) and $Rb_2Ga(B_5O_{10})(H_2O)_4$ (**3**) are insulators with optical band gaps around 4.48 and 3.54 eV, respectively (Figure S3 in the Supporting Information). IR studies indicate that they display absorption broad bands centered at 3240 and 3524 cm^{-1} due to the presence of hydroxyl groups or/and water molecules. In the case of **1**, the absorption bands centered at 1360 and 1240 cm^{-1} can be assigned to asymmetric stretching of the BO_3 group. The absorption bands centered at 1040 and 931 cm^{-1} can by assigned to the asymmetric stretch of the BO_4 group and symmetric stretch of the BO_3 group, respectively. The absorption bands at 711−799 cm^{-1} are attributable to the

dx.doi.org/10.1021/ic3006376 | Inorg. Chem. 2012, 51, 8810−8817

symmetric stretch of BO_4 groups. The absorption bands from 500 to 700 cm^{-1} are related to the stretching vibration of GaO_4 groups.[11b,i] Similar to **3**, the absorption bands at 1230−1390 cm^{-1} can be assigned to the asymmetric stretch of the BO_3 groups. The absorption peak centered at 1050 cm^{-1} can be assigned to the asymmetric stretch of the BO_4 group. The absorption peak centered at 940 cm^{-1} can be assigned to the symmetric stretch of the BO_3 group. The absorption bands at 726−808 cm^{-1} can be assigned to the symmetric stretch of BO_4 groups. The absorption bands from 500 to 700 cm^{-1} are related to the stretch vibration of GaO_4 groups.[11b] Since the bending modes of BO_4, GaO_4 polyhedron are likely to be significantly intermixed within the low-frequency vibrations, the absorption with frequency below 600 cm^{-1} is difficult to be assigned in detail (Figure S4 in the Supporting Information). These assignments are consistent with those previously reported.[11b,i,27] IR spectra confirmed the coexistence of BO_3, BO_4, and GaO_4 groups in **1** and **3**, consistent with the results obtained from crystallographic studies.

SHG Properties. Since the crystal structure of $Rb_2Ga(B_5O_{10})(H_2O)_4$ (**3**) is noncentrosymmetric, it is worthwhile to examine its SHG properties. SHG measurements on a Q-switched Nd:YAG laser with sieved powder samples (70−100 mesh) revealed that **3** displays a moderately strong SHG response approximately equal to that of KDP, giving further evidence of its noncentrosymmetric crystal structure (Figure 4a). Furthermore, the material is found to be phase matchable

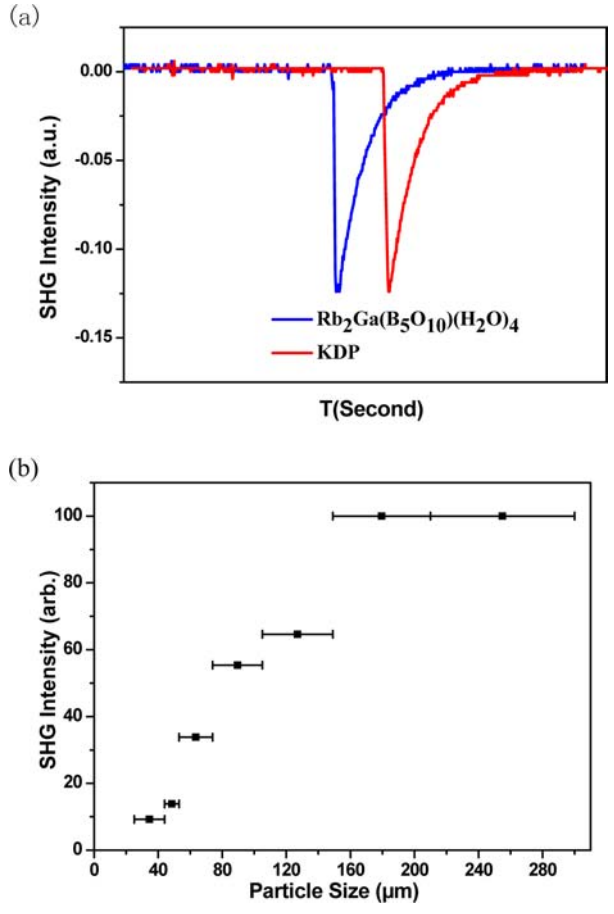

Figure 4. Comparison of the measured SHG response of $Rb_2Ga(B_5O_{10})(H_2O)_4$ (**3**) with that of KDP (a), and phase-matching curve for $Rb_2Ga(B_5O_{10})(H_2O)_4$ (**3**) (b).

(Figure 4b). According to the anionic-group theory, it is expected that its SHG signal mainly originated from the BO_3 groups as well as small contributions from BO_4 groups from the $[B_5O_{10}]^{5-}$ clusters.[28] The contributions from GaO_4 tetrahedra are expected to be very small since their distortions are very small.

Theoretical Studies. The calculated band structure of **3** along high-symmetry points of the first Brillouin zone is plotted in Figure 5. It is clear that both the lowest conduction band and

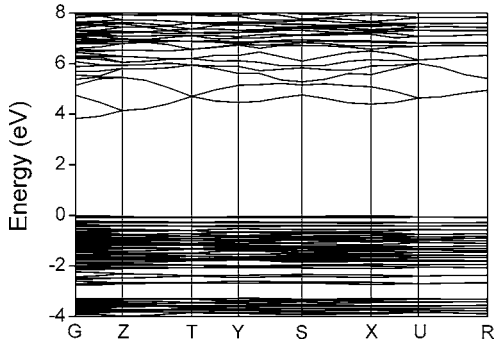

Figure 5. Calculated band structure of $Rb_2Ga(B_5O_{10})(H_2O)_4$ (**3**).

the highest valence band are localized at the G point, so **3** is a direct band gap material. The calculated band gap of 3.83 eV is very close to the experimental band gap of 3.76 eV. Hence, during subsequent optical calculations, no scissor operation was applied to modify the size of the electronic band gap.

The bands can be assigned according to the total and partial DOS, as plotted in Figure 6. The peaks localized around −23.5

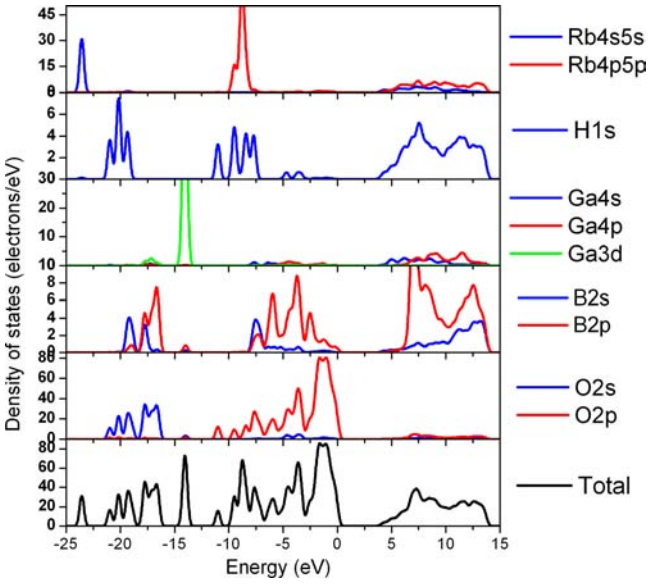

Figure 6. Electronic density of states of $Rb_2Ga(B_5O_{10})(H_2O)_4$ (**3**).

and −14.0 eV are contributed by isolated Rb-4s and Ga-3d states, respectively. The valence band in the range from −21.5 to −16.0 eV arises from mostly O-2s, mixing with a small amount of B-2s2p and H-1s states. In the vicinity of the Fermi level, namely, from −11.5 to 0 eV in the valence band and from 3.8 to 14.0 eV in the conduction band, the O-2p, B-2s2p, Ga-4s4p, and H-1s states are all involved and overlap fully among them, indicating the strong covalent interactions of B−O, Ga−

dx.doi.org/10.1021/ic3006376 | Inorg. Chem. 2012, 51, 8810−8817

O, and H−O bonds in the system. In addition, the peak around −8.8 eV in the Fermi level region is contributed by the isolated Rb-4p states.

The linear optical response properties of **3** were examined by calculating the complex dielectric function $\varepsilon(\omega) = \varepsilon_1(\omega) + i\varepsilon_2(\omega)$. Its imaginary part $\varepsilon_2(\omega)$ can be used to describe the real transitions between the occupied and the unoccupied electronic states. The imaginary part and real part of the frequency-dependent dielectric function of $Rb_2Ga(B_5O_{10})(H_2O)_4$ show obvious anisotropy along different dielectric axis directions (see Figures S5a and S5b in the Supporting Information). The curves of the averaged imaginary part and real part of dielectric function were obtained by $\varepsilon^{ave} = (\varepsilon_x + \varepsilon_y + \varepsilon_z)/3$ (see Figure S5c in the Supporting Information). The averaged imaginary part reveals the strongest adsorption peaks located at 8.3 and 17.7 eV, which can be mainly assigned to the electronic interband transitions from the O-2p to B-2p and a few Ga-4s4p states. The average static dielectric constant $\varepsilon(0)$ is 2.42. The dispersion of refractive index, calculated by the formula $n^2(\omega) = \varepsilon(\omega)$, indicates an order of $n^z > n^y \approx n^x$ in the low-photon energy range (Figure S6 in the Supporting Information), Obviously, the trend is very consistent with the real part of the dielectric function in the low-energy region (Figure S5b in the Supporting Information). It is notable that the difference of n^z and n^y (or n^x) is about 0.05 in the low-photon energy range (0−2.5 eV), which are big enough to realize phase matching. During second-harmonic generation, phase-match conditions, which ensure maximum conversion, can be achieved by ensuring that $|k_{2w}| = 2|k_w|$, that is, the fundamental and the second harmonic spread with the same refractive index in the crystal. According to our calculation, the values of n^x, n^y, and n^z are 1.55, 1.55, and 1.60 at 1064 nm and 1.56, 1.57, and 1.62 at 532 nm, respectively. It is obvious that the value of n^z at 1064 nm is larger than the value of n^y (or n^x) at 532 nm, which means that the phase-match condition for the SHG from 1064 to 532 nm can be satisfied when the fundamental and the second harmonic spread along a special direction but chose different polarizations in the crystal.

The space group of **3** belongs to class *222* and has three nonvanishing tensors of second-order susceptibility. Under the restriction of Kleinman's symmetry, only one independent SHG tensor d_{14} remains. The frequency-dependent d_{14} is plotted in Figure 7. The value of d_{14} at a wavelength of 1064 nm (1.165 eV) is 1.49×10^{-9} esu, which is very close to our experimental value of about that of KDP ($d_{36} = 1.1 \times 10^{-9}$ esu).

CONCLUSION

In summary, three novel galloborates, namely, $Ga\text{-}B_5O_8(OH)_2(en)_2{\cdot}H_2O$ (**1**), $LiGa(OH)(BO_3)(H_2O)$ (**2**), and $Rb_2Ga(B_5O_{10})(H_2O)_4$ (**3**), have been synthesized by hydrothermal reactions. Compound **1** with an infinite chain structure is the first example of a galloborate incorporating an organic component. This opens possibilities for synthesizing organically bonded galloborates with various structures and potentially useful properties. Both **2** and **3** crystallize in noncentrosymmetric space groups. The crystal structure of **2** exhibits a coordination layer composed of GaO_4, LiO_4, and BO_3 building units, whereas **3** displays a 3D anionic network based on GaO_4 tetrahedra and $[B_5O_{10}]^{5-}$ polyanions, forming tunnels in all three axial directions that accommodate the Rb^+ ions and solvated water molecules. Compound **3** displays moderate SHG efficiency comparable to that of KH_2PO_4. Furthermore, the material is found to be phase matchable. The present study showed that incorporation of gallium(III) oxide into the borate system not only enriches the structural chemistry of metal borates but also may afford new SHG materials. Our future research effort will be devoted to exploration of hydrothermal synthetic methods in generation of new types of inorganic and organically templated gallium borates.

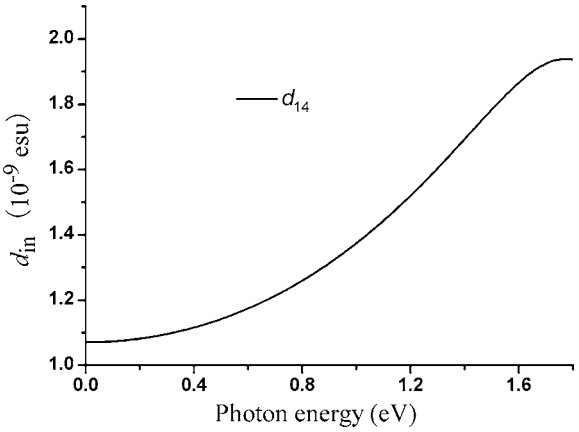

Figure 7. Calculated frequency-dependent second-harmonic generation coefficient for $Rb_2Ga(B_5O_{10})(H_2O)_4$ (**3**).

ASSOCIATED CONTENT

Supporting Information

X-ray crystallographic files in CIF format, simulated and measured XRD patterns, and UV−vis and IR spectra. This material is available free of charge via the Internet at http://pubs.acs.org.

AUTHOR INFORMATION

Corresponding Author

*E-mail: mjg@fjirsm.ac.cn (J.-G.M.); tcwmak@cuhk.edu.hk (T.C.W.M.).

Notes

The authors declare no competing financial interest.

ACKNOWLEDGMENTS

This work was supported partially by the National Natural Science Foundation of China (Grants 20825104 and 21001107). We gratefully acknowledge financial support by the Hong Kong Research Grants Council (GRF CUHK 402710) and the Wei Lun Foundation as well as the award of a Studentship to Ting Hu by The Chinese University of Hong Kong.

REFERENCES

(1) (a) Ok, K. M.; Chi, E. O.; Halasyamani, P. S. *Chem. Soc. Rev.* **2006**, *35*, 710. (b) Chen, C.-T.; Liu, G.-Z. *Annu. Rev. Mater. Sci.* **1986**, *16*, 203.

(2) (a) Becker, P. *Adv. Mater.* **1998**, *10*, 979. (b) Chen, C.; Wang, Y.; Wu, B.; Wu, K.; Zeng, W.; Yu, L. *Nature* **1995**, *373*, 322. (c) Hagerman, M. E.; Poeppelmeier, K. R. *Chem. Mater.* **1995**, *7*, 602.

(3) Chen, C.; Wu, Y.; Li, R. *J. Cryst. Growth* **1990**, *99*, 790.

(4) (a) Chang, H.-Y.; Kim, S.-H.; Halasyamani, P. S.; Ok, K. M. *J. Am. Chem. Soc.* **2009**, *131*, 2426. (b) Chang, H.-Y.; Kim, S.-H.; Ok, K. M.; Halasyamani, P. S. *J. Am. Chem. Soc.* **2009**, *131*, 6865. (c) Huang, H.; Yao, J.; Lin, Z.; Wang, X.; He, R.; Yao, W.; Zhai, N.; Chen, C. *Chem. Mater.* **2011**, *23*, 5457. (d) Pan, S.; Smit, J. P.; Watkins, B.; Marvelmpm, M. R.; Stern, C. L.; Poeppelmeier, K. R. *J. Am. Chem. Soc.*

2006, *128*, 11631. (e) Sun, C.-F.; Hu, C.-L.; Xu, X.; Ling, J.-B.; Hu, T.; Kong, F.; Long, X.-F.; Mao, J.-G. *J. Am. Chem. Soc.* **2009**, *131*, 9486.
(5) (a) Wang, S.; Ye, N.; Li, W.; Zhao, D. *J. Am. Chem. Soc.* **2010**, *132*, 8779. (b) Huang, H.-W.; Yao, J.-Y.; Lin, Z.-S.; Wang, X.-Y.; He, R.; Yao, W.-J.; Zhai, N.-X.; Chem, C. T. *Chem. Mater.* **2011**, *23*, 5457. (c) Huang, H.-W.; Yao, J.-Y.; Lin, Z.-S.; Wang, X.-Y.; He, R.; Yao, W.-J.; Zhai, N.-X.; Chem, C.-T. *Angew. Chem., Int. Ed.* **2011**, *123*, 9307.
(6) Huang, Y.-Z.; Wu, L.-M.; Wu, X.-T.; Li, L.-H.; Chen, L.; Zhang, Y.-F. *J. Am. Chem. Soc.* **2010**, *132*, 12788.
(7) Zhang, W.-L.; Cheng, W.-D.; Zhang, H.; Geng, L.; Lin, C.-S.; He, Z.-Z. *J. Am. Chem. Soc.* **2010**, *132*, 1508.
(8) Li, R.-K.; Yu, Y. *Inorg. Chem.* **2006**, *45*, 6840.
(9) Wang, S.; Ye, N. *Solid State Sci.* **2007**, *9*, 713.
(10) Barbier, J. *Solid State Sci.* **2007**, *9*, 344.
(11) (a) Barbier, J.; Penin, N.; Cranswick, L. M. *Chem. Mater.* **2005**, *17*, 3130. (b) Fan, H.; Wang, G.; Hu, L. *Solid State Sci.* **2009**, *11*, 2065. (c) Kissick, J. L.; Keszler, D. A. *Acta Crystallogr. C* **2000**, *56*, 631. (d) Park, H.; Barbier, J. *J. Solid State Chem.* **2000**, *155*, 354. (e) Park, H.; Barbier, J. *J. Solid State Chem.* **2000**, *154*, 598. (f) Park, H.; Barbier, J. *Acta Crystallogr. E* **2001**, *57*, i82. (g) Reshak, A.-H.; Chen, X.; Song, F.; Kityk, I. V.; Auluck, S. *J. Phys.: Condens. Matter* **2009**, *21*, 205402. (h) Smith, R. *Acta Crystallogr. C* **1995**, *51*, 547. (i) Subbalakshmi, P.; Veeraiah, N. *Mater. Lett.* **2002**, *56*, 880. (j) Yang, Z.; Chen, X.-L.; Liang, J.-K.; Zhou, T.; Xu, T. *J. Alloys Compd.* **2002**, *340*, 286. (k) Yang, Z.; Liang, J.-K.; Chen, X.-L.; Chen, J.-R. *J. Solid State Chem.* **2002**, *165*, 119. (l) Yang, Z.; Liang, J.-K.; Chen, X.-L.; Xu, T.; Xu, Y.-P. *J. Alloys Compd.* **2001**, *327*, 215. (m) Yu, Y.; Wu, Q.-S.; Li, R.-K. *J. Solid State Chem.* **2006**, *179*, 429.
(12) Cong, R.; Yang, T.; Li, K.; Li, H.; You, L.; Liao, F.; Wang, Y.; Lin, J. *Acta Crystallogr. B* **2010**, *66*, 141.
(13) Liu, Z.-H.; Yang, P.; Li, P. *Inorg. Chem.* **2007**, *46*, 2965.
(14) Wendlandt, W. M.; Hecht, H. G. *Reflectance Spectroscopy*; Interscience: New York, 1966.
(15) (a) Rieckhoff, K. E.; Peticolas, W. L. *Science* **1965**, *147*, 610. (b) Kurtz, S. K.; Perry, T. T. *J. Appl. Phys.* **1968**, *39*, 3798.
(16) *CrystalClear*, Version 1.3.5; Rigaku Corp.: Woodlands, TX, 1999.
(17) Sheldrick, G. M. *SHELXTL, Crystallographic Software Package*, Version 5.1; Bruker-AXS: Madison, WI, 1998.
(18) (a) Brown, I. D.; Altermatt, D. *Acta Crystallogr.B* **1985**, *41*, 244. (b) Brese, N. E.; O'Keeffe, M. *Acta Crystallogr. B* **1991**, *47*, 192.
(19) Spek, A. L. *PLATON*; Utrecht University: Utrecht, The Netherlands, 2001.
(20) (a) Segall, M. D.; Lindan, P. J. D.; Probert, M. J.; Pickard, C. J.; Hasnip, P. J.; Clark, S. J.; Payne, M. C. *J. Phys.: Condens. Matter* **2002**, *14*, 2717. (b) Milman, V.; Winkler, B.; White, J. A.; Pickard, C. J.; Payne, M. C.; Akhmatskaya, E. V.; Nobes, R. H. *Int. J. Quantum Chem.* **2000**, *77*, 895.
(21) Perdew, J. P.; Burke, K.; Ernzerhof, M. *Phys. Rev. Lett.* **1996**, *77*, 3865.
(22) Lin, J. S.; Qteish, A.; Payne, M. C.; Heine, V. *Phys. Rev. B* **1993**, *47*, 4174.
(23) Bassani, F.; Parravicini, G. P. *Electronic States and Optical Transitions In Solids*; Pergamon Press Ltd.: Oxford, 1975; 149.
(24) (a) Ghahramani, E.; Moss, D. J.; Sipe, J. E. *Phys. Rev. B* **1991**, *43*, 8990. (b) Ghahramani, E.; Moss, D. J.; Sipe, J. E. *Phys. Rev. Lett.* **1990**, *64*, 2815.
(25) (a) Duan, C.-G.; Li, J.; Gu, Z.-Q.; Wang, D.-S. *Phys. Rev. B* **1999**, *60*, 9435. (b) Guo, G.-Y.; Chu, K.-C.; Wang, D.-S.; Duan, C.-G. *Phys. Rev. B* **2004**, *69*, 205416. (c) Guo, G.-Y.; Lin, J.-C. *Phys. Rev. B* **2005**, *72*, 075416.
(26) (a) Wiesch, A.; Bluhm, K. *Acta Crystallogr. C* **1997**, 53−1730. (b) Ono, Y.; Nakaya, M.; Sugawara, T.; Watanabe, N.; Siraishi, H.; Komatsu, R.; Kajitani, T. *J. Cryst. Growth* **2001**, *229*, 472. (c) He, M.; Li, H.; Chen, X.; Xu, Y.; Xu, T. *Acta Crystallogr. C* **2001**, *57*, 1010. (d) Chen, X.; Li, M.; Zuo, J.; Chang, X.; Zang, H.; Xiao, W. *Solid State Sci.* **2007**, *9*, 678.
(27) (a) Zhang, J.-H.; Li, P.-X.; Mao, J.-G. *Dalton Trans.* **2010**, *39*, 5301. (b) Zhang, J.-H.; Kong, F.; Mao, J.-G. *Inorg. Chem.* **2011**, *50*, 3037.
(28) (a) Chen, C.-T.; Wu, Y.-C.; Li, R.-C. *J. Cryst. Growth.* **1990**, *99*, 790. (b) Yu, H.; Wu, H.; Pan, S.; Yang, Z.; Su, X.; Zhang, F. *J. Mater. Chem.* **2012**, *22*, 9665. (c) Yang, Y.; Pan, S.; Han, J.; Hou, X.; Zhou, Z.; Zhao, W.; Chen, Z.; Zhang, M. *Cryst. Growth Des.* **2011**, *11*, 3912. (d) Hu, C.-L.; Xu, X.; Sun, C.-F.; Mao, J.-G. J. *Phys.: Condens. Matter* **2011**, *23*, 395501.